



Comparative study of retinal nerve fibre layer thickness and retinal peripapillary capillary plexus microvascular vessel density: structure–function relationship analysis in glaucoma

Hayati Yilmaz¹ · Mehmet Talay Koçlu² · Alper Can Yılmaz² · Ali Hakan Durukan² · Atilla Bayer³ · Fatih Mehmet Mutlu²

Received: 11 August 2020 / Revised: 23 November 2020 / Accepted: 7 December 2020 / Published online: 19 January 2021

© The Author(s), under exclusive licence to The Royal College of Ophthalmologists 2021

Abstract

Background To investigate whether the retinal peripapillary capillary plexus vessel density (RPCP VD) or the retinal nerve fibre layer thickness (RNFLT) is better in showing the structure–function relationship in glaucoma.

Methods Sixty-seven patients with primary open-angle glaucoma (POAG) in one eye and no visual field loss in fellow eye were included in this study. The scans of RPCP VD and RNFLT, and the standard automated perimetry data [including mean deviation (MD), pattern standard deviation (PSD), sector-based pattern deviation (PD) values] were analysed and compared.

Results The global RNFLT was associated with MD ($P = 0.035$). RNFLTs of the superotemporal, superonasal, inferotemporal and inferonasal quadrants were associated with the corresponding PD ($P = 0.004, <0.001, 0.002$ and 0.012). The global RPCP VD was found to be associated with MD and PSD ($P = 0.030$ and 0.049 , respectively). RPCP VD of the superotemporal quadrant was associated with PD of the corresponding quadrant, as well as with PSD ($P = 0.003$ and 0.043 , respectively). Remaining RPCP VD values were only associated with the PD values of the corresponding quadrants ($P < 0.05$). The associations of the RPCP VD with PD were stronger than those of the RNFLT with PD [RPCP VD vs RNFLT: $R^2 = 0.624$ vs 0.558 ($P < 0.001$ for both) for the superotemporal, 0.649 vs 0.552 for the superonasal ($P < 0.001$ for both), 0.598 vs 0.427 for the inferotemporal ($P < 0.001$ for both), 0.581 vs 0.408 for the inferonasal ($P < 0.001$ for both), 0.594 vs 0.068 ($P < 0.001$ vs 0.098) for the temporal, and 0.338 vs 0.195 ($P < 0.001$ vs 0.004) for the nasal quadrants].

Conclusion In conclusion, the VD of RPCP was more informative in terms of the structure–function relationship in POAG. Future prospective follow-up studies with larger sample sizes are required to confirm the findings.

Introduction

The loss of retinal ganglion cells (RGC) caused by glaucoma can be reflected as diffuse or localised defects in the retinal nerve fibre layer (RNFL) [1, 2]. Alterations in RNFL have been associated with the indices of standard automatic

perimetry (SAP), which is still the gold standard method for visual field (VF) testing in the diagnosis and monitoring of glaucoma. Several studies have reported that structural defects often precede detectable VF loss as measured by SAP [3–6]. However, the structure–function relationship in glaucoma remains unclear due to the greater inter-individual variations [7–9]. Some researchers trying to establish this relationship have reported partial associations between RNFL and VF. In particular, the inferior and superior sectors of RNFL have been found to be more informative in detecting glaucomatous defects and progression [10–12].

Garway-Heath et al. [13] aimed to establish the structural relationship between the locations of VF and the corresponding regions of the optic nerve head (ONH), and created a sector-based VF and ONH map (G-H map), relating the 24–2 SAP test locations to the positions of the retinal nerve fibre

✉ Hayati Yilmaz
dr.hyilmaz@hotmail.com

¹ Department of Ophthalmology, Umraniye Training and Research Hospital, Health Sciences University, Istanbul, Turkey

² Department of Ophthalmology, Gulhane Medical Faculty, Health Sciences University, Ankara, Turkey

³ Dünyagöz Hospital, Kavaklıdere, Ankara, Turkey

bundles entry in ONH. The authors traced the RNFL defects and prominent bundles from each VF location towards ONH manually and obtained the position in degrees. Although this map was created based on structure, not function, it is still the only working map, which can be easily used in clinical practice [14]. However, for establishing the structure–function relationship, it is not sufficient to use optical coherence tomography (OCT) and measure RNFL as a structural parameter with the G-H map since the associations of the RNFL thickness with VF indices have been found to be stronger only in the inferior and superior quadrants [15].

The vascular theory of glaucoma pathogenesis postulates that RGC loss and therefore RNFL thinning is induced by the insufficient blood supply [16, 17]. Alterations in vessel morphology and hemodynamics have been reported and quantified using the retinal images of glaucomatous eyes [18]. In particular, decreased macular and peripapillary vessel density (VD) have been demonstrated in glaucomatous eyes based on the assessment of OCT-angiography (OCT-A) images, which is an enhancement of traditional OCT [19, 20]. In addition, the lower parapapillary choroidal VD has been found to be associated with future VF progression [21, 22]. If the vascular theory is right, VD measurements using OCT-A could give more reliable information about the structure–function relationship than RNFL analysis. Therefore, in this study, we aimed to investigate whether the microvascular VD of the retinal peripapillary capillary plexus (RPCP) or the RNFL thickness was better in showing the structure–function relationship.

Materials and methods

Demographic data and clinical findings

This study was carried out in accordance with the principles of the Declaration of Helsinki after obtaining the approval of the Non-Interventional Clinical Research Ethics Committee of the Health Sciences University, Turkey. The files of 3014 patients who presented to the outpatient glaucoma clinics of the Ophthalmology Department of Gulhane Medical Faculty between January 2019 and February 2020 were retrospectively screened. Included in the study were patients with a diagnosis of primary open-angle glaucoma (POAG) and primary juvenile glaucoma (PJG) in at least one eye and with no detectable glaucomatous VF defects in the contralateral eye, who had undergone a complete ophthalmological examination, including LogMAR-converted best-corrected visual acuity (BCVA) and intra-ocular pressure (IOP) measurements, slit-lamp biomicroscopy, and non-dilated funduscopy along with VF testing (Humphrey Field Analyzer II, Humphrey-Zeiss Instruments, Dublin, CA, USA), RNFL analysis, and OCT-A scans (AngioVue,

Optovue Inc., Fremont, CA, USA) during the same visit. The diagnosis of POAG and PJG was made in accordance with the Terminology and Guidelines for Glaucoma of the European Glaucoma Society [23]. Increased IOP (>21 mmHg), presence of acquired characteristic glaucomatous changes of ONH, presence of glaucomatous VF defects and open-angle were accepted as the typical features of POAG and PJG. The exclusion criteria were age under 18 years, refractive error of $\geq \pm 3$ dioptres, LogMAR-converted BCVA of >0.5 (<0.3 in decimals), presence of any other ophthalmological pathology (e.g., diabetes or hypertensive retinal diseases, amblyopia, optic nerve abnormalities, optic neuropathies other than glaucoma and age-related macular degeneration) or a history of ocular surgery (including cataract and glaucoma surgery) or a systemic disease (e.g., diabetes mellitus, rheumatologic disorders) that could confound the assessment results, OCT-A signal strength of <70, presence of glaucomatous damage in both eyes and SAP low test reliability ($\geq 20\%$ fixation losses and false-negative errors, and $\geq 15\%$ false-positive errors).

Only 112 of 3014 patients had OCT-A, RNFL and SAP tests at the same visit. Sixty-seven of those 112 patients with glaucoma were included in this study. Forty-five patients were excluded from the study due to having glaucomatous damage in both eyes ($n = 31$), having a history of ocular surgery ($n = 10$) or having a systemic disease ($n = 4$).

The eyes with obvious glaucomatous VF defects were included in the glaucomatous eyes group and the contralateral eyes with no detectable VF defects were included in the fellow eyes group.

Standard automatic perimetry

A Humphrey field analyser II (Humphrey-Zeiss Instruments) was used to analyse VF. The mean deviation (MD, dB) and pattern standard deviation (PSD, dB) indices of VF were recorded for each eye. Then, the VF pattern deviation (PD) numeric map was divided into superotemporal, superonasal, inferotemporal, inferonasal, nasal and temporal quadrants based on the anatomical relation established by Garway-Heath et al. [13]. Sectoral PD was calculated manually, with regard to the sectoral PD, this was represented by the mean value of all points for each sector on the PD map of the VF output (Fig. 1A).

RNFL and peripapillary microvascular VD measurements

OCT-A scans were obtained using an AngioVue OCT-A system (Optovue Inc.) with an A-scan rate of 70,000/s using a light source of 840 nm. En face images were acquired focusing ONH (4.5 mm \times 4.5 mm) using the Angio Disc QuickVue module. Each scan consisted of 400 \times 400

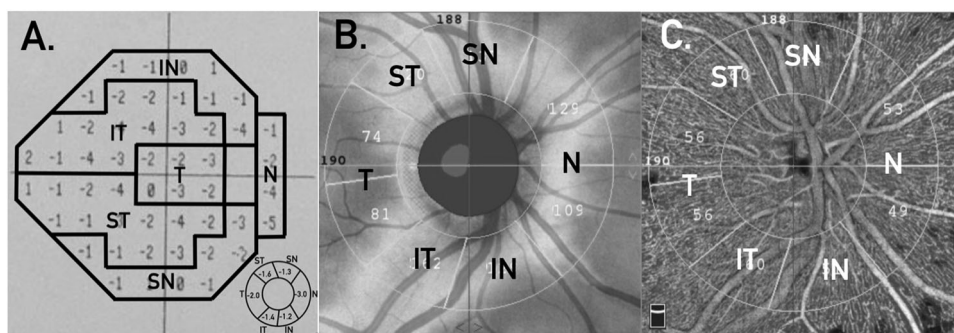


Fig. 1 An example from study subjects. **A** A pattern deviation numeric map that stratified in to six quadrants in accordance with the Garway-Heath Map [13]. **B** The retinal nerve fibre layer thickness analysis of the same eye. **C** The retinal peripapillary capillary plexus

microvascular vessel density analysis of the same eye. ST superotemporal, SN superonasal, IT inferotemporal, IN inferonasal, T temporal, N nasal.

A-scans with two following B-scans at each fixed location. To reduce motion artefacts, each scan comprised one orthogonal horizontal and vertical scan. The device provides data on the anatomic Bruch membrane opening–based neuroretinal rim and ONH, RNFL thickness and the VD of RPCP in a single scan. The device’s software automatically removes the large vessels from the images and gives the microvascular VD values of the scanned area. After scanning, the RNFL thicknesses of the superotemporal, superonasal, inferotemporal, inferonasal, nasal and temporal quadrants along with the corresponding microvascular VDs of RPCP were recorded for statistical analyses (Fig. 1B, C). The device’s scan quality value (OCT-A signal strength) was also recorded for each subject to investigate the effects of the scan quality.

Statistical analyses

SPSS v. 21 (SPSS, Inc., Chicago, IL, USA) was used for statistical analyses. Quantitative variables were defined as mean and standard deviation, and qualitative variables as percentages. The generalised estimating equation (GEE) analysis was used to compare the eye-related parameters, namely IOP, RNFL and RPCP-VD measurements between the glaucomatous and fellow eyes of the study participants. A GEE model with a working correlation matrix “independent” was created for each eye parameter (BCVA, IOP, VF indices, RNFL and RPCP VD values) as a dependent variable, and the group of the individual was taken as the main effect (ordinal factor). A curve estimation regression analysis was performed between RPCP VD and RNFL quadrants vs corresponding PD quadrants for the glaucomatous and fellow eyes separately, and scatterplots were created with linear and second-order regression slopes for each parameter. The results of the curve-estimating regression analysis were given with R^2 and P values. In the glaucomatous eyes, after collinearity diagnostics, the age,

gender and OCT-A signal strength corrected associations of the RPCP VD and RNFL measurements with VF indices were sought by creating a final linear regression model for each quadrant of the RPCP VD and RNFL measurements as dependent variables and the VF indices as covariates. The results of these regression models were given with the regression coefficient (B), 95% confidence interval and P values. A P value of less than 0.05 was considered statistically significant.

Results

Demographic data and clinical findings

The demographic and clinical features of the study participants, including the mean RNFL thicknesses, microvascular VDs of RPCP and VF indices are presented in Table 1. Thirty-seven (55%) of the study participants were female. All the patients were Caucasian. The mean age of the patients was 63.18 ± 13.55 years. All the patients were older than 35 years, and all of them were diagnosed as POAG.

The mean LogMAR-converted BCVA was 0.0 ± 0.0 for the fellow eyes and 0.27 ± 0.22 for the glaucomatous eyes. The main reason for the reduction of visual acuity was glaucoma. The difference in IOP was significant between the fellow and glaucomatous eyes, with the mean IOP value being calculated as 14.13 ± 3.09 and 17.83 ± 3.94 , respectively ($P = 0.009$, GEE).

The MD and mean PSD were -8.68 ± 6.72 and 5.70 ± 3.71 dB, respectively, for the glaucomatous eyes, and -1.88 ± 1.88 and 1.67 ± 0.33 dB, respectively, for the fellow eyes. The difference was significant for both MD and PSD ($P < 0.001$ for both, GEE). The difference of the sector-based PD values of the SAP between the glaucomatous and fellow eyes were also significant ($P < 0.001$ for all quadrants, GEE).

Table 1 Demographic and clinical findings of the study participants.

	Fellow Eyes (n = 67)	Glaucomatous Eyes (n = 67)	P*
Age (years ± SD)	63.18 ± 13.55		n/a
Female (%)	55		n/a
BCVA (LogMAR ± SD)	0.0 ± 0.0	0.27 ± 0.22	<0.001
IOP (mmHg ± SD)	14.13 ± 3.09	17.83 ± 3.94	0.009
SAP data			
MD (dB ± SD)	-1.88 ± 1.88	-8.68 ± 6.72	<0.001
PSD (dB ± SD)	1.67 ± 0.33	5.70 ± 3.71	<0.001
PD, supt q. (dB ± SD)	-1.75 ± 0.51	-5.80 ± 5.14	<0.001
PD, supn q. (dB ± SD)	-1.78 ± 0.54	-5.54 ± 4.97	<0.001
PD, infnt q. (dB ± SD)	-1.76 ± 0.68	-6.05 ± 5.09	<0.001
PD, infn q. (dB ± SD)	-1.80 ± 0.59	-5.76 ± 5.64	<0.001
PD, tem q. (dB ± SD)	-1.48 ± 0.89	-2.62 ± 2.90	<0.001
PD, nas q. (dB ± SD)	-2.04 ± 1.26	-4.45 ± 3.62	<0.001
RNFLT			
Global (µm ± SD)	100.33 ± 14.68	85.15 ± 21.88	<0.001
Supt q. (µm ± SD)	130.06 ± 31.92	112.34 ± 33.34	<0.001
Supn q. (µm ± SD)	100.32 ± 23.83	87.12 ± 29.01	<0.001
Inft q. (µm ± SD)	139.35 ± 32.75	115.58 ± 36.18	<0.001
Infn q. (µm ± SD)	102.12 ± 22.84	88.30 ± 30.24	<0.001
Tem q. (µm ± SD)	70.59 ± 10.63	72.00 ± 29.15	0.187
Nas q. (µm ± SD)	89.08 ± 18.33	77.96 ± 22.18	<0.001
RPCP VD			
Global (% ± SD)	50.35 ± 4.36	43.61 ± 9.36	<0.001
Supt q. (% ± SD)	52.13 ± 4.54	41.09 ± 10.98	<0.001
Supn q. (% ± SD)	50.24 ± 5.12	40.78 ± 11.12	<0.001
Inft q. (% ± SD)	51.45 ± 4.98	42.18 ± 10.79	<0.001
Infn q. (% ± SD)	51.22 ± 5.01	40.25 ± 11.56	<0.001
Tem q. (% ± SD)	52.65 ± 4.65	48.97 ± 8.22	<0.001
Nas q. (% ± SD)	47.21 ± 5.65	41.03 ± 9.70	<0.001

Significant *P* values are shown in bold.

SD standard deviation, *BCVA* best-corrected visual acuity, *IOP* intra-ocular pressure, *MD* mean deviation, *PSD* pattern standard deviation, *PD* pattern deviation, *Supt* superotemporal, *q* quadrant, *Supn* superonasal, *Inft* inferotemporal, *Infn* inferonasal, *Tem* temporal, *Nas* nasal, *RNFLT* retinal nerve fibre layer thickness, *RPCP* retinal peripapillary capillary plexus, *VD* vessel density.

*The results of the generalised estimating equations.

The RNFLs of all quadrants were significantly thinner in the glaucomatous eyes compared to the fellow eyes, except for the temporal quadrant ($P = 0.187$ for the temporal quadrant and $P < 0.001$ for the remaining quadrants, GEE). In all quadrants, the microvascular VDs of RPCP were significantly reduced in the glaucomatous eyes compared to the fellow eyes ($P < 0.001$ for all quadrants, GEE).

Scatterplots; glaucomatous vs fellow eyes and RPCP microvascular VD vs RNFL thickness

Figure 2 presents the scatterplots of the fellow eyes' RNFL thickness and RPCP microvascular VD for all quadrants against the corresponding PD values. Figure 3 presents the

same scatterplots of the glaucomatous eyes. For all the curve-estimating regression analyses, the second-order (quadratic) regression model was found to be a better fit than the linear regression model. However, this difference between the regression models did not affect statistical significance in any quadrant.

In the fellow eyes, the RPCP microvascular VD was found to be associated with the corresponding PD only for the superotemporal, superonasal and temporal quadrants (for the second-order regression model; superotemporal quadrant: $R^2 = 0.166$, $P < 0.001$; superonasal quadrant: $R^2 = 0.214$, $P < 0.001$; temporal quadrant: $R^2 = 0.085$, $P = 0.009$, respectively). For the remaining analyses, the PD values did not have any other association with the

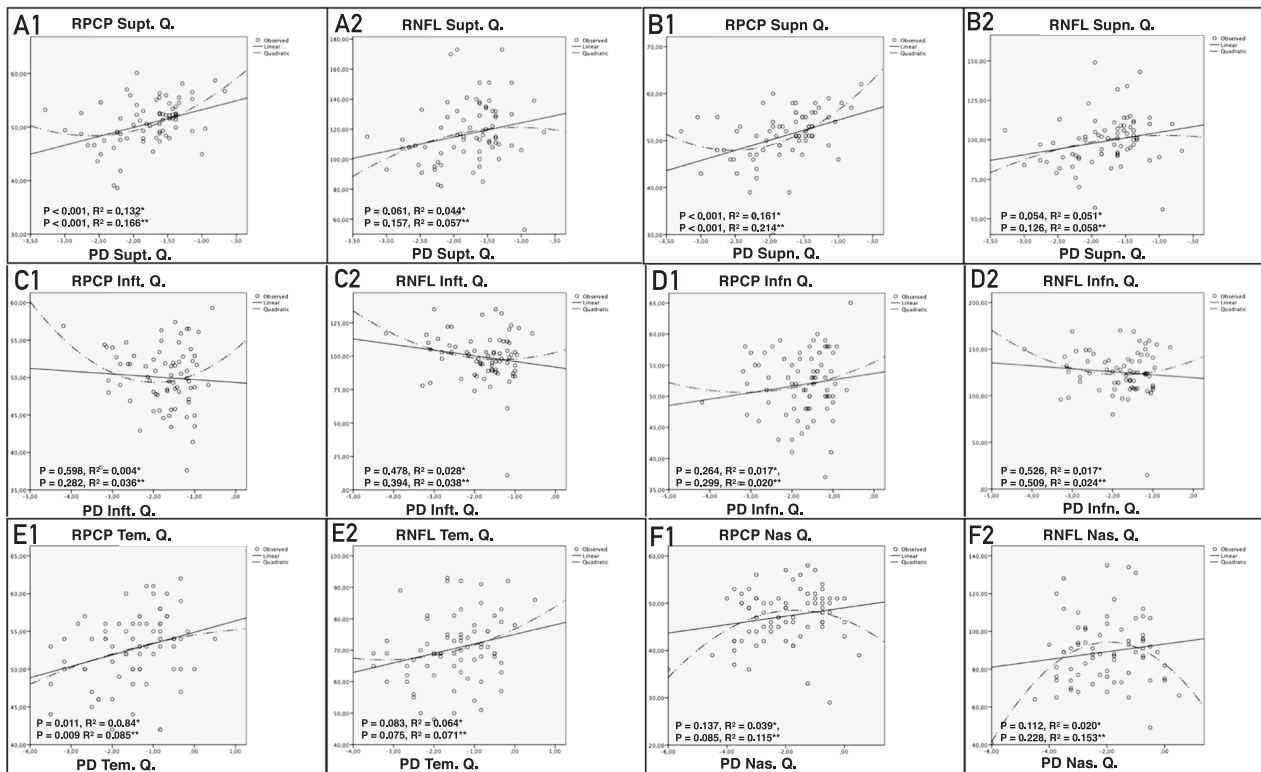


Fig. 2 Scatterplots of the fellow eyes' RNFL thickness and RPCP microvascular VD for all quadrants against the corresponding PD values. **A1, A2** Scatterplots of the superotemporal quadrant. **B1, B2** Scatterplots of the superonasal quadrant. **C1, C2** Scatterplots of the inferotemporal quadrant. **D1, D2** Scatterplots of the inferonasal quadrant. **E1, E2** Scatterplots of the temporal quadrant. **F1, F2** Scatterplots of the nasal quadrant. **A1, B1, C1, D1, E1, F1** RPCP

microvascular VD against PD. **A2, B2, C2, D2, E2, F2** RNFL thickness against PD. RPCP retinal peripapillary capillary plexus, RNFL retinal nerve fibre layer, PD pattern deviation, Q quadrant, Supt superotemporal, Supn superonasal, Inft inferotemporal, Infn inferonasal, Tem temporal, Nas; nasal, VD vessel density. *The P and R^2 values of the linear regression models. **The P and R^2 values of the quadratic (second-order) regression models.

RNFL thickness ($P = 0.157, 0.126, 0.394, 0.509, 0.083$ and 0.228 for the superotemporal, superonasal, inferotemporal, inferonasal, temporal and nasal quadrants, respectively) or the RPCP microvascular VD values ($P = 0.282, 0.472$ and 0.085 for the inferotemporal, inferonasal and nasal quadrants, respectively). However, except for the RNFL thickness of the temporal quadrant, regression analyses revealed strong associations between all the PD values with the RNFL thickness and RPCP microvascular VDs of the corresponding quadrants in the glaucomatous eyes (RNFL thickness with PD: $P < 0.001$ for the superotemporal, superonasal, inferotemporal and inferonasal quadrants and $P = 0.098$ and 0.004 for the temporal and nasal quadrants, respectively; RPCP microvascular VD with PD; $P < 0.001$ for all quadrants). In the eyes with glaucoma, the associations of the RPCP microvascular VD with PD were stronger than those of the RNFL thickness with PD (RPCP microvascular VD vs RNFL thickness: $R^2 = 0.624$ vs 0.558 for the superotemporal quadrant, 0.649 vs 0.552 for the superonasal quadrant, 0.598 vs 0.427 for the inferotemporal quadrant, 0.581 vs 0.408 for the inferonasal quadrant, 0.594

vs 0.068 for the temporal quadrant and 0.338 vs 0.195 for the nasal quadrant).

The final regression models

The associations of the RNFL thickness with the SAP data are given in Table 2 for all quadrants. The global RNFL thickness was found to be associated only with MD ($P = 0.035$) and the RNFL thicknesses of the superotemporal, superonasal, inferotemporal and inferonasal quadrants were only associated with the corresponding PD ($P = 0.004, < 0.001, 0.002$ and 0.012 , respectively). The RNFL thicknesses of the temporal and nasal quadrants did not have an association with any of the SAP parameters ($P > 0.05$ for all).

The associations of the RPCP microvascular VD with the SAP data are given in Table 3 for all quadrants. The global RPCP microvascular VD was found to be associated with MD and PSD ($P = 0.030$ and 0.049 , respectively). The RPCP microvascular VD of the superotemporal quadrant was associated with the PD of the corresponding quadrant,

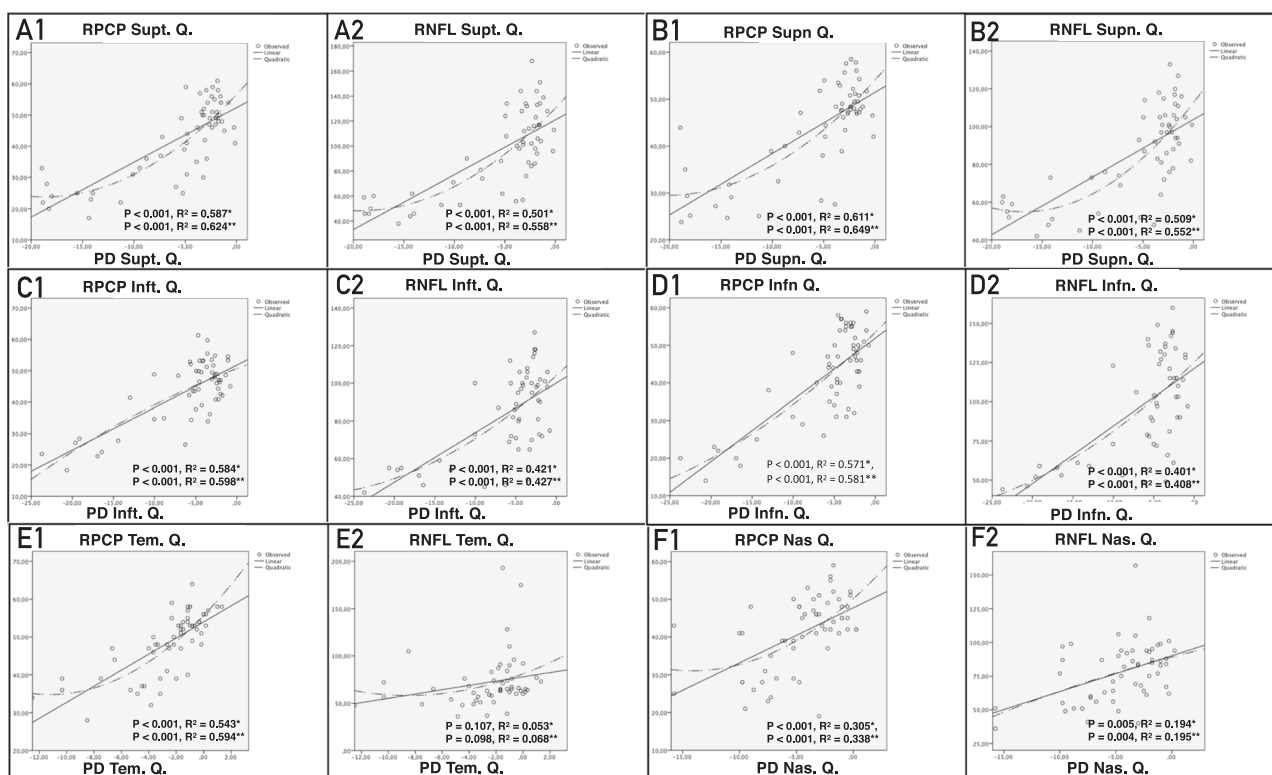


Fig. 3 Scatterplots of the glaucomatous eyes' RNFL thickness and RPCP microvascular VD for all quadrants against the corresponding PD values. **A1, A2** Scatterplots of the superotemporal quadrant. **B1, B2** Scatterplots of the superonasal quadrant. **C1, C2** Scatterplots of the inferotemporal quadrant. **D1, D2** Scatterplots of the inferonasal quadrant. **E1, E2** Scatterplots of the temporal quadrant. **F1, F2** Scatterplots of the nasal quadrant. **A1, B1, C1, D1, E1, F1** RPCP

microvascular VD against PD. **A2, B2, C2, D2, E2, F2** RNFL thickness against PD. RPCP retinal peripapillary capillary plexus, RNFL retinal nerve fibre layer, PD pattern deviation, Q quadrant, Supt superotemporal, Supn superonasal, Inft inferotemporal, Infn inferonasal, Tem temporal, Nas nasal, VD vessel density. *The P and R^2 values of the linear regression models. **The P and R^2 values of the quadratic (second-order) regression models.

as well as with the PSD ($P = 0.003$ and 0.043 , respectively). The superonasal, inferotemporal, inferonasal and temporal RPCP microvascular VD values were associated with the PD values of the corresponding quadrants ($P = 0.001$, 0.001 , 0.002 and < 0.001 , respectively). The inferonasal quadrant's RPCP microvascular VD was also found associated with the PD of the inferotemporal quadrant ($P = 0.031$). However, the RPCP microvascular VD of the nasal quadrant was not associated with any of the SAP parameters ($P > 0.05$, for all).

Discussion

The purpose of this retrospective cross-sectional study was to investigate whether the RNFL thickness or the RPCP microvascular VD was better in showing the structure–function relationship. We compared healthy eyes with glaucomatous eyes after stratifying VF into six quadrants in accordance with the G-H map [13], and we searched for the associations of VF indices with both the RNFL thickness and the RPCP microvascular VD. Both

parameters were found to be associated with the sectoral VF indices in the eyes with glaucoma; however, in almost all quadrants, the RPCP microvascular VD better fit the sectoral VF loss than the RNFL thicknesses.

The OCT scanning of RNFL, ganglion cell complex and macula has been an important part of the diagnosis and monitoring of glaucoma for over a decade [7, 24]. However, SAP remains the gold standard method for this purpose. The ability to detect progression by SAP and OCT is significantly influenced by the stage of glaucoma. While OCT is the most valuable method for the early stages, SAP is more useful in the late stages [24]. Iester et al. [10] and Gunderson et al. [11] both found that the superior and inferior quadrants are more informative in the diagnosis and follow-up of glaucoma. These findings are similar to our study, in which we found that the RNFL thicknesses of all quadrants, except for the temporal quadrant, were associated with the VF loss of the corresponding sector according to the separate curve-estimating regression method; however, after the multivariate regression analysis, the association for the nasal quadrant disappeared while that of the superotemporal, superonasal, inferotemporal and

Table 2 The associations of the RNFLT profile with the SAP data in the glaucomatous eyes. (n = 67).

	B / 95% CI / P						
	Global RNFLT	RNFLT, <i>supt. q.</i>	RNFLT, <i>supn. q.</i>	RNFLT, <i>inft. q.</i>	RNFLT, <i>infn. q.</i>	RNFLT, <i>tem. q.</i>	RNFLT, <i>nas. q.</i>
MD	0.689 0.055/1.733 0.035	0.752 −0.089/2.403 0.094	0.697 −0.068/2.183 0.089	0.675 −0.101/1.914 0.103	0.599 −0.129/1.991 0.109	0.584 −0.612/1.780 0.339	0.556 −0.437/1.540 0.272
PSD	−1.963 −5.300/0.074 0.064	−2.743 −6.605/0.104 0.097	−2.803 −7.001/0.113 0.091	−4.004 −7.909/0.089 0.081	−3.991 −8.012/0.093 0.079	−0.272 −3.808/3.265 0.880	−0.764 −1.943/0.788 0.372
PD of the <i>supt. q.</i>	1.001 −0.432/2.578 0.118	1.456 0.314/2.768 0.004	1.211 −0.019/2.718 0.056	0.910 −0.712/2.089 0.172	0.811 −0.919/1.789 0.202	1.002 −0.593/2.653 0.174	1.287 −0.097/2.781 0.092
PD of the <i>supn. q.</i>	0.919 −0.198/2.512 0.103	1.197 −0.021/2.654 0.061	1.513 0.579/3.015 <0.001	0.992 −0.645/2.314 0.171	0.912 −0.707/2.109 0.219	0.961 −0.642/1.919 0.197	0.891 −0.421/1.991 0.231
PD of the <i>inft. q.</i>	0.519 −1.191/2.014 0.716	−0.213 −1.314/0.762 0.841	−0.671 −1.909/0.917 0.794	1.412 0.214/3.101 0.002	1.234 −0.001/2.896 0.050	−1.075 −3.145/1.876 0.219	0.623 −0.782/2.009 0.195
PD of the <i>infn. q.</i>	0.545 −1.104/3.453 0.516	−0.317 −1.691/0.368 0.419	−0.661 −2.174/0.689 0.612	1.191 −0.045/2.118 0.084	1.245 0.104/2.836 0.012	−0.937 −1.998/0.514 0.348	0.578 −0.692/1.870 0.514
PD of the <i>tem. q.</i>	0.739 −1.219/2.697 0.451	0.712 −1.903/3.123 0.554	0.814 −1.896/3.451 0.505	0.401 −2.101/3.356 0.415	0.397 −1.756/3.001 0.386	2.490 −0.002/4.982 0.050	0.941 −0.718/2.601 0.266
PD of the <i>nas. q.</i>	−0.239 −1.860/1.389 0.772	−0.371 −2.109/1.500 0.687	−0.425 −2.593/1.216 0.571	−1.251 −3.485/0.701 0.182	−0.849 −3.102/1.318 0.283	0.064 −2.476/2.604 0.961	1.215 −0.721/3.459 0.134

Significant *P* values are shown in bold.

RNFLT retinal nerve fibre layer thickness, *SAP* standard automated perimetry, *B* coefficient, *CI* confidence interval, *supt* superotemporal, *q* quadrant, *supn* superonasal, *inft* inferotemporal, *infn* inferonasal, *tem* temporal, *nas* nasal, *MD* mean deviation, *PSD* pattern standard deviation, *PD* pattern deviation.

inferonasal quadrants remained. It is known that there is a significant structure–function relationship between RNFL and VF [15, 25], but this relationship is not perfect [15]. In addition, due to the presence of large inter-individual variations, the associations between the RNFL parameters and SAP indices are limited for prediction [2].

Several studies have investigated the retinal microvascular network in patients with glaucoma and reported that VD is decreased and retinal blood flow is reduced in the hemiretina corresponding to the affected hemifield [19, 20, 26–28]. Yarmohammadi et al. [29] arrived at the same conclusion with an additional finding that VD decreased in eyes with glaucoma diffusely, not only in the hemiretina of the affected hemifield, but also in the intact hemiretina, which supports the vascular theory of the glaucoma pathogenesis and underlines the importance of vascular alterations in glaucoma progression. In our study, the microvascular VDs of RPCP were found to be associated with the PD values in all corresponding quadrants in the

glaucomatous eyes. However, the association initially found for the nasal quadrant disappeared after the multivariate regression analysis. Furthermore, the associations of RPCP microvascular VDs with PD were greater than those of the RNFL thickness with PD. This finding suggests that the microvascular network data are better at defining the structure–function relationship than RNFL thickness measurements. In the literature, the only study similar to ours was conducted by Sakaguchi et al. [30] but with two main methodological differences: first, instead of PD, they used the sensitivity values obtained from SAP testing for sector-based comparisons, and second, they utilised two different devices for scanning VD and RNFL. However, the main results of the two studies are the same, both showing that the VD data are much more associated with the sector-based SAP data than RNFL measurements.

Despite strong associations of the RPCP microvascular VD with the PD values of the corresponding VF sector in our study, the structure–function relationship was not

Table 3 The associations of the RPCP VDs with the SAP data in the glaucomatous eyes (n = 67).

	B / 95% CI / P						
	Global RPCP VD	RPCP VD, supt. q.	RPCP VD, supn. q.	RPCP VD, infn. q.	RPCP VD, infn. q.	RPCP VD, tem. q.	RPCP VD, nas. q.
MD	0.398 0.040/0.756 0.030	0.451 −0.009/0.871 0.054	0.509 −0.007/0.904 0.061	0.395 −0.081/0.796 0.102	0.401 −0.083/0.847 0.114	0.557 −0.045/0.854 0.453	0.301 −0.156/0.192 0.098
PSD	−0.833 −1.981/0.003 0.049	−1.391 −2.278/−0.009 0.043	−1.345 −2.108/0.014 0.052	−1.216 −2.489/0.056 0.061	−1.219 −2.577/0.032 0.071	−0.428 −1.235/0.379 0.291	−0.815 −2.059/0.398 0.472
PD of the supt q.	0.314 −0.245/0.801 0.309	0.882 0.225/1.493 0.003	0.784 −0.009/1.117 0.062	−0.198 −0.843/0.476 0.490	−0.214 −0.910/0.315 0.455	−0.061 −0.331/0.446 0.685	0.232 −0.245/0.701 0.341
PD of the supn q.	0.299 −0.258/0.819 0.314	0.701 −0.002/1.252 0.059	0.904 0.341/1.507 0.001	−0.151 −0.899/0.686 0.701	−0.182 −0.904/0.599 0.687	−0.062 −0.349/0.146 0.686	0.233 −0.377/0.802 0.471
PD of the infn q.	0.298 −0.203/0.801 0.211	−0.332 −0.891/0.311 0.239	−0.402 −1.173/0.349 0.352	1.023 0.465/1.582 0.001	0.998 0.021/1.497 0.031	−0.281 −0.667/0.132 0.221	0.231 −0.374/0.891 0.322
PD of the infn q.	0.333 −0.191/0.924 0.262	−0.299 −0.873/0.299 0.301	−0.194 −0.683/0.176 0.388	0.807 −0.023/1.401 0.073	1.105 0.343/1.707 0.002	−0.222 −0.576/0.132 0.214	0.280 −0.263/0.812 0.314
PD of the tem q.	0.508 −0.165/1.181 0.136	−0.119 −0.915/0.577 0.712	−0.208 −1.102/0.605 0.659	0.205 −0.603/1.091 0.556	0.223 −0.722/1.342 0.495	1.682 1.118/2.246 <0.001	0.225 −0.622/1.072 0.596
PD of the nas q.	−0.287 −0.835/0.261 0.267	−0.081 −0.703/0.644 0.850	−0.100 −0.841/0.992 0.813	−0.803 −1.042/0.115 0.102	−0.687 −1.003/0.214 0.238	−0.476 −0.530/0.057 0.135	−0.079 −0.604/0.762 0.817

Significant *P* values are shown in bold.

RPCP retinal peripapillary capillary plexus, VD vessel density, SAP standard automated perimetry, B coefficient, CI confidence interval, supt superotemporal, q quadrant, supn superonasal, infn inferotemporal, infn inferonasal, tem temporal, nas nasal, MD mean deviation, PSD pattern standard deviation, PD pattern deviation.

perfect. It has been a real problem for ophthalmologists to obtain the exact structure–function relationship due to the nature of testing modalities [31]. Several scientists have developed VF maps to explain this relationship [31–35]. In this study, we used the map developed by Garway-Heath et al. [13]. The differences in such maps prove the difficulty of obtaining the true structure–function relationship. Using the G-H map, the lowest correlations of the VF points with the ONH sectors are observed in the nasal quadrant, as Gardiner et al. [33] found in their study. For this reason, the authors stated that the structure–function relationship was not reliable for the nasal sector. This can also be the reason why the association between nasal quadrant's RPCP microvascular VD and the PD of the nasal quadrant was not significant in this study. Therefore, we consider that using disc-centred VF testing to reveal the structure–function relationship can provide more reliable data in future studies.

This study has several limitations. The first concerns the retrospective and cross-sectional design, which made it almost impossible to draw definitive conclusions. Also, as a result of the retrospective design, we did not investigate the systemic arterial blood pressure that is very important since this study is about peripapillary vascular network changes in patients with glaucoma. In addition, a potential sample selection bias could be in question because of the retrospective design and the limited sample size of this study. Prospective follow-up studies are needed to provide an understanding of the role of vascular alterations in glaucoma pathogenesis and progression. Secondly, we did not stratify the glaucomatous eyes of the study participants in accordance with the VF loss patterns nor did we exclude eyes with severe glaucoma. Another limitation is that the fellow eyes of the sample were accepted as the control group of the glaucomatous eyes; however, we cannot accept them as completely healthy since some may have been pre-perimetric

glaucomatous. Accordingly, the VDs and RNFL thicknesses of truly healthy eyes may provide different results compared to the evaluation of fellow eyes. Therefore, future studies with healthy control groups are needed. In addition, our results would have been much more reliable if we had analysed only the eyes with localised VF loss and sought associations of VF with the VD and RNFL thickness of the corresponding sector. Lastly, we did not analyse the effects of glaucoma and systemic medication used by the patients. These medications could alter the microvascular circulation of the retina, and therefore it may have affected our results.

In conclusion, the microvascular VD of RPCP was more informative in terms of the structure–function relationship in POAG. However, our suggestions are subjective due to lack of statistical analysis that could actually compare the performance of RNFL thickness and RPCP microvascular VD. Although, similar to the RNFL thickness, the relationship of the structural RPCP microvascular VD with functional SAP testing was not perfect, OCT-A is a promising tool that can assist in the clinical management of vascular alterations in glaucoma, and it can theoretically improve our understanding of the pathophysiology of the disease, especially its underlying vascular mechanism.

Summary

What was known before

- The associations of the RNFL thickness with VF indices have been found to be stronger only in the inferior and superior quadrants, and RNFL analysis was not perfect in terms of showing structure–function relationship in POAG.

What this study adds

- The microvascular VD of RPCP was more informative than RNFL thickness in terms of the structure–function relationship in POAG. However, the relationship of RPCP small VD with VF testing was also not perfect, as it was with the RNFL thickness.

Author contributions Hypothesis and concept: HY, AB; Design: HY, MTK, AHD, FMM; Organisation: HY, AB; Data collection: ACY, MTK; Statistics: HY; Article preparation and interpretation: HY; Critical review of the article: AB, MTK, AHD, FMM.

Compliance with ethical standards

Conflict of interest The authors declare that they have no conflict of interest.

Publisher's note Springer Nature remains neutral with regard to jurisdictional claims in published maps and institutional affiliations.

References

1. Reus NJ, Lemij HG. The relationship between standard automated perimetry and GDx VCC measurements. *Investig Ophthalmol Vis Sci.* 2004;45:840–5. <https://doi.org/10.1167/iops.03-0646>
2. Lan YW, Henson DB, Kwartz AJ. The correlation between optic nerve head topographic measurements, peripapillary nerve fibre layer thickness, and visual field indices in glaucoma. *Br J Ophthalmol.* 2003;87:1135–41. <https://doi.org/10.1136/bjo.87.9.1135>
3. Bagga H, Greenfield DS. Quantitative assessment of structural damage in eyes with localized visual field abnormalities. *Am J Ophthalmol.* 2004;137:797–805. <https://doi.org/10.1016/j.ajo.2003.11.060>
4. Bagga H, Greenfield DS, Knighton RW. Macular symmetry testing for glaucoma detection. *J Glaucoma.* 2005;14:358–63. <https://doi.org/10.1097/01.jgg.0000176930.21853.04>
5. Choi J, Cho Hsoo, Lee CH, Kook MS. Scanning laser polarimetry with variable corneal compensation in the area of apparently normal hemifield in eyes with normal-tension glaucoma. *Ophthalmology.* 2006;113:1954–60. <https://doi.org/10.1016/j.opth.2006.05.040>
6. Grewal DS, Sehi M, Greenfield DS. Diffuse glaucomatous structural and functional damage in the hemifield without significant pattern loss. *Arch Ophthalmol.* 2009;127:1442–8. <https://doi.org/10.1001/archophthalmol.2009.196>
7. Kim NR, Lee ES, Seong GJ, Kim JH, An HG, Kim CY. Structure–function relationship and diagnostic value of macular ganglion cell complex measurement using Fourier-domain OCT in glaucoma. *Invest Ophthalmol Vis Sci.* 2010;51:4646–51. <https://doi.org/10.1167/iops.09-5053>
8. Pollet-Villard F, Chiquet C, Romanet JP, Noel C, Aptel F. Structure–function relationships with spectral-domain optical coherence tomography retinal nerve fiber layer and optic nerve head measurements. *Investig Ophthalmol Vis Sci.* 2014;55:2953–62. <https://doi.org/10.1167/iops.13-13482>
9. Casado A, Cerveró A, López-De-Eguileta A, Fernández R, Fonseca S, González JC, et al. Topographic correlation and asymmetry analysis of ganglion cell layer thinning and the retinal nerve fiber layer with localized visual field defects. *PLoS One.* 2019;14:1–14. <https://doi.org/10.1371/journal.pone.0222347>
10. Iester M, Swindale NV, Mikelberg FS. Sector-based analysis of optic nerve head shape parameters and visual field indices in healthy and glaucomatous eyes. *J Glaucoma.* 1997;6:370–6. <https://doi.org/10.1097/00061198-199712000-00006>
11. Gundersen KG, Heijl A, Bengtsson B. Optic nerve head sector analysis recognizes glaucoma most effectively around disc poles. *Acta Ophthalmol Scand.* 1999;77:13–8. <https://doi.org/10.1034/j.1600-0420.1999.770103.x>
12. Emdadi A, Kono Y, Sample PA, Maskaleris G, Weinreb RN. Parapapillary atrophy in patients with focal visual field loss. *Am J Ophthalmol.* 1999;128:595–600. [https://doi.org/10.1016/S0002-9394\(99\)00189-0](https://doi.org/10.1016/S0002-9394(99)00189-0)
13. Garway-Heath DF, Poinoosawmy D, Fitzke FW, Hitchings RA. Mapping the visual field to the optic disc in normal tension glaucoma eyes. *Ophthalmology.* 2000;107:1809–15. [https://doi.org/10.1016/S0161-6420\(00\)00284-0](https://doi.org/10.1016/S0161-6420(00)00284-0)
14. Hood DC, Kardon RH. A framework for comparing structural and functional measures of glaucomatous damage. *Prog Retin Eye Res.* 2007;26:688–710. <https://doi.org/10.1016/j.preteyeres.2007.08.001>

15. Bowd C, Zangwill LM, Medeiros FA, Tavares IM, Hoffmann EM, Bourne RR, et al. Structure–function relationships using confocal scanning laser ophthalmoscopy, optical coherence tomography, and scanning laser polarimetry. *Invest Ophthalmol Vis Sci.* 2006;47. <https://doi.org/10.1167/iovs.05-1489>
16. Chan KKW, Tang F, Tham CCY, Young AL, Cheung CY. Retinal vasculature in glaucoma: a review. *BMJ Open Ophthalmol.* 2017;1:e000032. <https://doi.org/10.1136/bmjophth-2016-000032>
17. Yarmohammadi A, Zangwill LM, Diniz-Filho A, Suh MS, Yousefi S, Saunders LJ, et al. Relationship between optical coherence tomography angiography vessel density and severity of visual field loss in glaucoma. *Ophthalmology.* 2016;123:2498–508. <https://doi.org/10.1016/j.ophtha.2016.08.041>
18. Orlando JI, Barbosa Breda J, van Keer K, Blaschko MB, Blanco PJ, Bulant CA. Towards a glaucoma risk index based on simulated hemodynamics from fundus images. In: *Lecture notes in computer science (including subseries lecture notes in artificial Intelligence and lecture notes in Bbioinformatics)*; 2018. https://doi.org/10.1007/978-3-030-00934-2_8
19. Wu J, Sebastian RT, Chu CJ, McGregor F, Dick AD, Liu L. Reduced macular vessel density and capillary perfusion in glaucoma detected using OCT angiography. *Curr Eye Res.* 2019;44:533–40. <https://doi.org/10.1080/02713683.2018.1563195>
20. Lommatzsch C, Rothaus K, Koch JM, Heinz C, Grisanti S. OCTA vessel density changes in the macular zone in glaucomatous eyes. *Graefe's Arch Clin Exp Ophthalmol.* 2018;256:1499–508. <https://doi.org/10.1007/s00417-018-3965-1>
21. Park HYL, Shin DY, Jeon SJ, Park CK. Association between parapapillary choroidal vessel density measured with optical coherence tomography angiography and future visual field progression in patients with glaucoma. *JAMA Ophthalmol.* 2019;137:681–8. <https://doi.org/10.1001/jamaophthalmol.2019.0422>
22. Na KI, Lee WJ, Kim YK, Jeoung JW, Park KH. Evaluation of optic nerve head and peripapillary choroidal vasculature using swept-source optical coherence tomography angiography. *J Glaucoma.* 2017;26:665–8. <https://doi.org/10.1097/IJG.0000000000000684>
23. European Glaucoma Society Terminology and Guidelines for Glaucoma, 4th Edition—Chapter 2. Classification and terminology supported by the EGS Foundation. *Br J Ophthalmol.* 2017;101:73–127. <https://doi.org/10.1136/bjophthalmol-2016-EGSguideline.002>
24. Tatham AJ, Medeiros FA. Detecting structural progression in glaucoma with optical coherence tomography. *Ophthalmology.* 2017;124:S57–S65. <https://doi.org/10.1016/j.ophtha.2017.07.015>
25. Leung CK, Chong KK, Chan W, Yiu CK, Tso M, Woo J, et al. Comparative study of retinal nerve fiber layer measurement by StratusOCT and GDx VCC, II: structure/function regression analysis in glaucoma. *Invest Ophthalmol Vis Sci.* 2005;46:3702–11. <https://doi.org/10.1167/iovs.05-0490>
26. Sehi M, Goharian I, Konduru R, Tan O, Srinivas S, Sadda SR, et al. Retinal blood flow in glaucomatous eyes with single-hemifield damage. *Ophthalmology.* 2014;121:750–8. <https://doi.org/10.1016/j.ophtha.2013.10.022>
27. Mansoori T, Sivaswamy J, Gamalapati JS, Balakrishna N. Radial peripapillary capillary density measurement using optical coherence tomography angiography in early glaucoma. *J Glaucoma.* 2017;26:438–43. <https://doi.org/10.1097/IJG.0000000000000649>
28. Zhang S, Wu C, Liu L, Jia Y, Zhang Y, Zhang Y, et al. Optical coherence tomography angiography of the peripapillary retina in primary angle-closure glaucoma. *Am J Ophthalmol.* 2017;182:194–200. <https://doi.org/10.1016/j.ajo.2017.07.024>
29. Yarmohammadi A, Zangwill LM, Diniz-Filho A, Saunders LJ, Suh MH, Wu Z, et al. Peripapillary and macular vessel density in patients with glaucoma and single-hemifield visual field defect. *Ophthalmology.* 2017;124:709–19. <https://doi.org/10.1016/j.ophtha.2017.01.004>
30. Sakaguchi K, Higashide T, Udagawa S, Ohkubo S, Sugiyama K. Comparison of sectoral structure-function relationships in glaucoma: vessel density versus thickness in the peripapillary retinal nerve fiber layer. *Investig Ophthalmol Vis Sci.* 2017;58:5251–62. <https://doi.org/10.1167/iovs.17-21955>
31. Ferreras A, Pablo LE, Garway-Heath DF, Fogagnolo P, García-Feijoo J. Mapping standard automated perimetry to the peripapillary retinal nerve fiber layer in glaucoma. *Investig Ophthalmol Vis Sci.* 2008;49:3018–25. <https://doi.org/10.1167/iovs.08-1775>
32. Asaoka R, Russell RA, Malik R, Crabb DP, Garway-Heath DF. A novel distribution of visual field test points to improve the correlation between structure-function measurements. *Investig Ophthalmol Vis Sci.* 2012;53:8396–404. <https://doi.org/10.1167/iovs.12-9794>
33. Gardiner SK, Johnson CA, Cioffi GA. Evaluation of the structure-function relationship in glaucoma. *Invest Ophthalmol Vis Sci.* 2005;46:3712–7. <https://doi.org/10.1167/iovs.05-0266>
34. McKendrick AM, Denniss J, Wang YX, Jonas JB, Turpin A. The proportion of individuals likely to benefit from customized optic nerve head structure–function mapping. *Ophthalmology.* 2017;124:554–61. <https://doi.org/10.1016/j.ophtha.2016.12.016>
35. Garway-Heath DF, Holder GE, Fitzke FW, Hitchings RA. Relationship between electrophysiological, psychophysical, and anatomical measurements in glaucoma. *Investig Ophthalmol Vis Sci.* 2002;43:2213–20.